The 1998 Midwest Symposium on Circuits and Systems, University of Notre Dame, August 1998

Generalized-Eigenfilter Design of a Hybrid FIR/Analog Receive Filter Minimizing ISI, ACI, and Gaussian Noise

Jeffrey O. Coleman
Dan P. Scholnik*

jeffc@alum.mit.edu
scholnik@radar.nrl.navy.mil

Naval Research Laboratory
Radar Division
Washington, DC

Abstract

The flexibility and design power inherent in the generalized-eigenfilter approach to sophisticated least-squares FIR-filter design problems is here demonstrated by using it to address a classic problem: the MMSE design of a (nonadaptive) fractional-tap-spacing linear equalizer and matched filter. The solution accounts for the analog filters and minimizes a combination of noise variance, mean-square intersymbol interference (ISI), and mean-square adjacent-channel interference (ACI).

1. Introduction

The now classic eigenfilter method of FIR-filter optimization [1–3] associates the desired optimum filter with the minimum-eigenvalue eigenvector of a positive-definite matrix whose structure embodies the filter specifications. Replacing the eigenproblem involved with a generalized eigenproblem provides a fundamentally more-powerful approach [4, 5] by generalizing the equality constraint inherent in these methods. This generalization enables design of embedded filters [4], it permits the elimination [5] of the distortion associated with fixing the response at some reference frequency in the ordinary eigenfilter methods, it permits true least-squares design [6], and because it effects a constrained optimization, it permits some problems to be easily solved that cannot quite be handled even with classic "true least-squares" design.

This particular paper addresses the design of a communications filter, but its purpose is less to champion a particular receive-filter design approach than to suggest through example that the generalized-eigenfilter concept is an FIR-filter design tool simple and flexible enough to be applied by nonspecialists to challenging applications.

2. Problem statement

The design process is one of mathematically formulating and minimizing the error power in the hypothetical test system of Fig. 1. The baseband-equivalent communication system in the dashed box includes the nonlinear-phase filter "h_k" that will be designed here along with a transmitter, a channel with additive Gaussian noise and adjacent-channel interference (ACI), a pre-decision receive filter, a sampler, and an output decimator. Random process d_k comprises data symbols input to the system and to a parallel gain/delay path below it that provides uncorrupted reference symbols for comparison in determining error. (This path exists only on paper and for purposes of design.) Independent and wide-sense stationary random processes model the symbol stream, noise, and ACI. In this formulation all three can be characterized by arbitrary power spectra. The error-signal power $P_{\text{err}} = P_a + P_i + P_n$ then is a sum of mean-square errors due to ACI, ISI, and noise. The filter h_k is designed here by minimizing error power P_{err}.

System parameters and filters except the FIR-filter h_k under design are presumed chosen earlier on suitable general principles. The analog pre-filter $g(t)$ might, for example, contribute to the required out-of-band signal suppression while contributing in-band signal distortion to a degree presumably easily equalized in FIR filter response h_k.

In the classic formulation of this equalizer design problem (not involving eigenfilter methods), the system gain q in the lower path would be simply a constant, the *desired* system gain. Here instead it is the *actual* system gain—it is a linear function of the filter coefficients being optimized (details to follow). Because of this, the data process d_k will drive the power-measurement input through an impulse re-

*Scholnik's involvement in this work was supported by National Science Foundation grant MIP-9896034 to the University of Maryland Baltimore County, where he is a graduate student and where Coleman is an Adjunct Assistant Professor of Computer Science and Electrical Engineering.

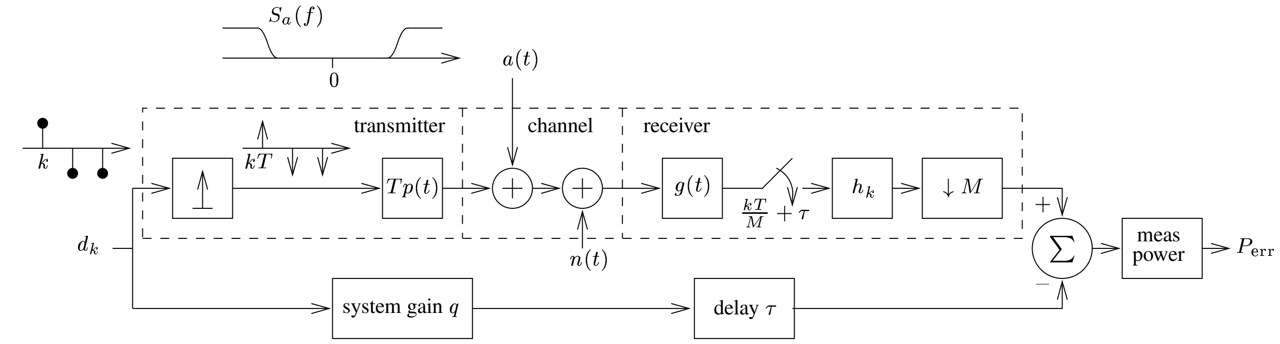

Figure 1. A hypothetical error-measurement test system for the communication system in the dashed box.

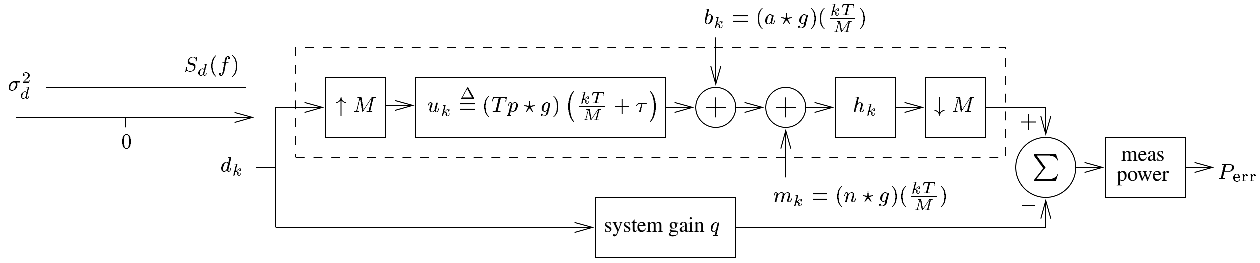

Figure 2. This (multirate) discrete-time system is equivalent to the continuous-/discrete-time hybrid of Fig. 1.

sponse that is strictly linear in the weights of the filter h_k under design, and this linearity is the key to eigenfilter formulation. The desired system gain must still be specified, but this is done below using the one quadratic constraint both permitted and required by the generalized-eigenfilter method.

3. Generalized-eigenfilter formulation

The system is first reduced in steps to a simpler form that the optimization setup can directly mirror. The analog components of Fig. 1 are accommodated by incorporating them into an equivalent, purely discrete-time system as shown in Figure 2. Notationally, function $h \star g$ is the convolution of functions h and g, and $(h \star g)(t)$ is the value of that function at time t (similarly in discrete time). Wide-sense stationary processes b_k and m_k represent ACI and noise respectively after prefiltering and sampling. In the single-rate equivalent in Fig. 3, output powers P_a, P_n, and P_i, due to ACI, noise, and ISI power are then determined separately. System gain q is finally explicitly stated.

The block diagram of Fig. 3 leads to the pseudocode of Fig. 4, which parallels nearly line for line the actual code used to carry out the design in our rapid-prototype `scilab` implementation. The data structures in $\mathbf{d}$, $\mathbf{b}$, and $\mathbf{m}$ contain the precomputed spectral information that will be needed later to compute samples of the corresponding processes' autocorrelations. The triangles suggest the shape of the basis functions used here for the piecewise-linear spectral

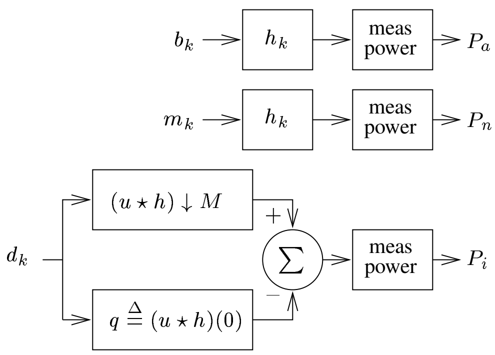

Figure 3. Single-rate equivalent of Fig. 2.

$$
\begin{aligned}
\mathbf{d} &= \textbf{Process}(\Delta, [1]) \\
\mathbf{b} &= \textbf{Process}(\Delta, \texttt{ManySbSamples}) \\
\mathbf{m} &= \textbf{Process}(\Delta, \texttt{ManySmSamples}) \\
u &= \textbf{Sequence}(\texttt{PrecomputedCoeffs}) \\
\delta &= \textbf{Sequence}([1]) \\
\mathbf{h} &= \textbf{optSequence}(13) \\
\mathbf{q} &= (u \star \mathbf{h})(0) \\
P_d &= \textbf{Power}(\mathbf{d}) \\
\mathbf{P}_a &= \textbf{Power}(\mathbf{b} \star \mathbf{h}) \\
\mathbf{P}_n &= \textbf{Power}(\mathbf{m} \star \mathbf{h}) \\
\mathbf{P}_i &= \textbf{Power}(\mathbf{d} \star ((u \star \mathbf{h}) \downarrow M - \mathbf{q}\,\delta))
\end{aligned}
$$

$$\text{minimize } (\mathbf{P}_a + \mathbf{P}_i + 10^{-3}\mathbf{P}_n)/P_d \text{ with } |\mathbf{q}|^2 = 1$$

Figure 4. Optimization of filter h_k of Fig. 3.

approximations from which exact autocorrelation samples are computed with an FFT technique [4]. Precomputed data structures u and δ represent fixed impulse-response sequences, the filtered and sampled transmit pulse from Fig. 2 and an ordinary unit sample function respectively. Those sequences are scalar, but here data structure $\mathbf{h}$ represents a vector sequence,

$$
\begin{array}{rccccc}
n = & 0 & 1 & 2 & \cdots & N-1 \\
\mathbf{h}(n) = & \begin{pmatrix} 1 \\ 0 \\ 0 \\ 0 \\ \vdots \\ 0 \end{pmatrix} & \begin{pmatrix} 0 \\ 1 \\ 0 \\ 0 \\ \vdots \\ 0 \end{pmatrix} & \begin{pmatrix} 0 \\ 0 \\ 1 \\ 0 \\ \vdots \\ 0 \end{pmatrix} & \ddots & \begin{pmatrix} 0 \\ 0 \\ 0 \\ 0 \\ \vdots \\ 1 \end{pmatrix}
\end{array}
$$

(zero elsewhere) relating the still-unknown optimization variables, in vector $\mathbf{x}$ say, to the corresponding to-be-optimized impulse response h_k through the implicit linear relationship $h_k = \mathbf{x}^T\mathbf{h}(k)$.

These particular unit-vector choices for $\mathbf{h}(k)$ lead to $h_k = x_1, x_2, \ldots, x_N$ for $n = 0, \ldots, N-1$, so that the optimization variables represent the weights of an FIR filter h_k of length N. Other vector sequences $\mathbf{h}(k)$ could be constructed instead [4] to make the variables represent the symmetrically placed weights of a linear-phase filter, the spread-out weights of a halfband filter, the real and imaginary parts of complex filter weights, or a combination of these or other structural features. In this design, however, a nonlinear-phase filter is called for because the group delay of analog pre-filter $g(t)$ will require equalization.

System gain q is implicity represented in a similar way by vector $\mathbf{q}$ through $q = \mathbf{x}^T\mathbf{q}$, though here representation vector $\mathbf{q}$ is computed rather than directly specified in the way that $\mathbf{h}$ was.

Computations determining various system powers are next in Fig. 4. Power P_d is a scalar (used later for normalization) and is computed in the ordinary way through spectral integration, but data structures $\mathbf{P}_a$, $\mathbf{P}_n$, and $\mathbf{P}_i$ actually relate the corresponding average powers to the optimization variables. Each of those average powers P in Fig. 4 is specified as the power in the process resulting from the convolution of some impulse response, say $f(n) = \mathbf{x}^T\mathbf{f}(n)$, with some input random process, say with autocorrelation $R(n)$. Because the impulse response is linear in the optimization variables, the power becomes quadratic in those variables and is given by [4] quadratic form $P = \mathbf{x}^T\mathrm{Re}\{[\mathbf{f}(n) \star R(n) \star \mathbf{f}^H(-n)]_{n=0}\}\mathbf{x}$. Data structures $\mathbf{P}_a$, $\mathbf{P}_n$, and $\mathbf{P}_i$ therefore actually contain the kernel matrices of quadratic forms determined in this way.

The last line in Fig. 4 specifies minimization of a normalized sum of powers that is a quadratic form in the optimization variables and represented here by the corresponding normalized sum of the three kernel matrices. This minimization is subject to the requirement that the system gain have unit magnitude. Notation $|\mathbf{q}|^2$ refers implicitly to $|q|^2 = \mathbf{x}^T\mathrm{Re}\{\mathbf{q}\mathbf{q}^H\}\mathbf{x}$, represented internally by the kernel matrix on its right side. Finally then, the problem has been reduced to the minimization of some $\mathbf{x}^T\mathbf{Q}\mathbf{x}$ subject to the constraint $\mathbf{x}^T\mathbf{G}\mathbf{x} = 1$ for appropriate known kernel matrices $\mathbf{Q}$ and $\mathbf{G}$. (The latter is singular, of rank one).

Recall that if $\beta\mathbf{Q}\psi = \alpha\mathbf{G}\psi$ then scalar ratio α/β and vector ψ are a generalized eigenvalue and the associated generalized eigenvector respectively for the pair of real symmetric matrices $(\mathbf{Q}, \mathbf{G})$. If $\beta = 0$, the generalized eigenvalue is infinite. A version of the Rayleigh principle states that $\min_{\mathbf{x}}\{\mathbf{x}^T\mathbf{Q}\mathbf{x} : \mathbf{x}^T\mathbf{G}\mathbf{x} = 1\}$ is equal to the minimum generalized eigenvalue and that the minimizing vector $\mathbf{x}$ is the associated generalized eigenvector appropriately scaled. Thus with a standard library routine we can find the optimal $\mathbf{x}$ and indirectly the optimal $h_k = \mathbf{x}^T\mathbf{h}(k)$ but including an unpredictable rotation in the complex plane associated with the indeterminate complex phase of our weak system-gain constraint $|q|^2 = 1$. This rotation is easily corrected after the fact.

3.1. Comparison with true least squares

As an aside, note that if system gain q were not the actual gain but were instead the desired system gain, a constant, then this would be a true least-squares problem and solvable by solving a linear system in the usual way. The needed constraint of the actual system gain to equal the desired one is linear and could be incorporated algebraically. Thus the problem setup here demonstrates an approach that is basically applicable to either method, neither of which has a significant computational advantage. The two methods will similarly be equally applicable whenever the kernel matrix in the quadratic form in the equality constraint of the generalized-eigenfilter method is of rank one. But when it is of higher rank, no true least-squares equivalent will exist. Therefore the generalized-eigenfilter approach is actually the more powerful.

4. A numerical design example

In this example the transmit pulse shape $Tp(t)$ corresponds to a root raised cosine $P(f)$ with 35% excess bandwidth relative to signaling rate $1/T$. Adjacent-channel spectral shapes are the same as in the primary channel but are centered at $\pm1.5/T$. The analog portion of the receive filtering, with frequency response $G(f)$, is a third-order Butterworth lowpass filter with an arbitrarily chosen cutoff frequency of $1/(2T)$. Magnitude $|G(f)|$ contributes significantly to the desired root raised-cosine shape, easing the requirements on the FIR filter. The nonlinear-phase FIR filter operates at an oversampling rate of $M = 4$ with 13 real coefficients h_k, to be optimized. Sampling epoch τ is chosen here as the sum of the DC group-delay of the analog filter and half the FIR filter length (a choice that could likely be improved upon through numerical experiment).

The optimized coefficients for h_k in Table 1 lead to the system pulse $\sum_k h_k(Tp \star g)(t + \tau - kT/M)$ is shown in Fig. 5, and Figure 6 shows the key frequency responses. In the optimization the trade-off between the three performance measures was managed through the weighting of the three powers in the objective. Here the spectral noise level was set for $E_s/N_0 = 1$, so in the objective function the noise power was scaled by 10^{-3} to a more realistic level. Speaking loosely, the weights applied to the three powers affect the "pressure" applied towards the three goals in the optimization, but those pressures meet different levels of "resistance," so the numerical values of the weights do not directly correspond to the relative levels of the three powers in the solution. The optimized P_a and P_i levels were 48.1 dB and 41.6 dB below signal level P_d, and the optimized P_n was such that the noise penalty relative to the ideal matched filter was 0.07 dB.

.0125534
−.0533546
−.0562742
−.0106553
.1628778
.3226365
.3728486
.2432388
.0634882
−.0590976
−.0428689
−.0038856
.0482568

Table 1. Optimized filter coefficients h_k.

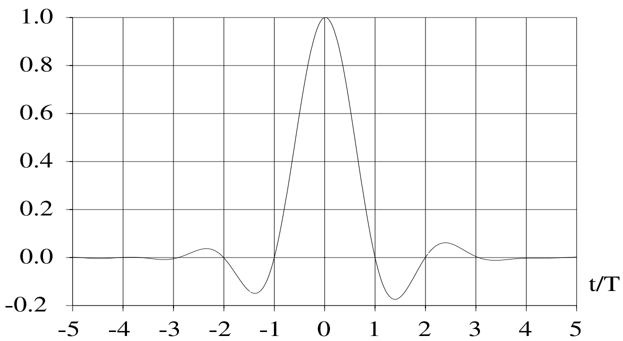

Figure 5. Optimized equivalent system pulse.

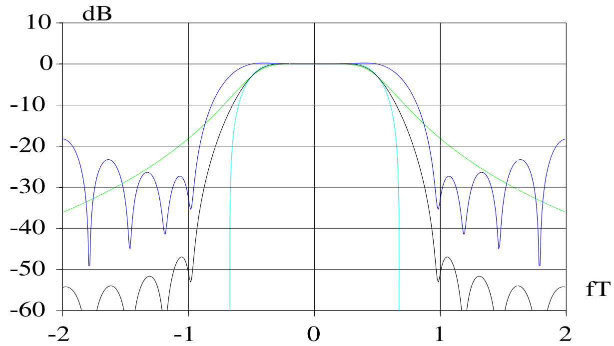

Figure 6. The key frequency responses of the numerical example, on the left edge moving down: FIR response $H(fT/M)$, analog response $G(f)$, and optimized cascade response $H(fT/M)G(f)$, with ideal response $P(f)$ in the center.

References

[1] P. P. Vaidyanathan and Truong Q. Nguyen, "Eigenfilters: A new approach to least-squares FIR filter design and applications including Nyquist filters," *IEEE Trans. on Circuits and Systems*, vol. CAS-34, no. 1, pp. 11–23, Jan. 1987.

[2] Soo-Chang Pei and Jong-Jy Shyu, "Complex eigenfilter design of arbitrary complex coefficient FIR digital filters," *IEEE Trans. on Circuits and Systems II*, vol. CAS-40, no. 1, pp. 32–39, Jan. 1993.

[3] Truong Q. Nguyen, "The design of arbitrary FIR digital filters using the eigenfilter method," *IEEE Trans. on Signal Processing*, vol. 41, no. 3, pp. 1128–1139, Mar. 1993.

[4] Jeffrey O. Coleman, "Embedded FIR generalized eigenfilters using test inputs," in *Proc. Int'l Conf. on Acoustics, Speech, and Signal Processsing (ICASSP '98)*, May 1998.

[5] J. O. Coleman, "Quadratic FIR-filter design as a generalized eigenproblem," in *Proc. 1998 Eureopean Signal Processing Conference (EUSIPCO '98)*, Sept. 1998, to be presented.

[6] J. O. Coleman, "True least-squares FIR-filter design using a generalized-eigenfilter method," *IEEE Trans. Circuits and Systems II*, submitted.